MYELOID NEOPLASIA

Loss of *Asxl1* leads to myelodysplastic syndrome–like disease in mice

Jiapeng Wang,[1,2] Zhaomin Li,[1,2] Yongzheng He,[1,2] Feng Pan,[1,2,3] Shi Chen,[1,2] Steven Rhodes,[1,2] Lihn Nguyen,[1,2] Jin Yuan,[1,2] Li Jiang,[1,2] Xianlin Yang,[1,2] Ophelia Weeks,[3] Ziyue Liu,[4] Jiehao Zhou,[5] Hongyu Ni,[6] Chen-Leng Cai,[7] Mingjiang Xu,[1,2,8] and Feng-Chun Yang[1,2,9]

[1]Department of Pediatrics, and [2]Herman B. Wells Center for Pediatric Research, Indiana University School of Medicine, Indianapolis, IN; [3]Department of Biological Sciences, Florida International University, Miami, FL; [4]Department of Biostatistics, and [5]Department of Pathology and Laboratory Medicine, Indiana University School of Medicine, Indianapolis, IN; [6]Department of Pathology and Laboratory Medicine, University of Calgary, Calgary, AB, Canada; [7]Department of Developmental and Regenerative Biology, the Mindich Child Health and Development Institute, Icahn School of Medicine at Mount Sinai, New York, NY; and [8]Department of Medical and Molecular Genetics, and [9]Department of Anatomy and Cell Biology, Indiana University School of Medicine, Indianapolis, IN

Key Points

- Deletion/haploinsufficiency of *Asxl1* causes MDS-like disease in mice.
- *Asxl1* loss reduces the HSC pool and decreases HSC hematopoietic repopulating capacity in vivo.

***ASXL1* is mutated/deleted with high frequencies in multiple forms of myeloid malignancies, and its alterations are associated with poor prognosis. De novo *ASXL1* mutations cause Bohring-Opitz syndrome characterized by multiple congenital malformations. We show that *Asxl1* deletion in mice led to developmental abnormalities including dwarfism, anophthalmia, and 80% embryonic lethality. Surviving *Asxl1*$^{-/-}$ mice lived for up to 42 days and developed features of myelodysplastic syndrome (MDS), including dysplastic neutrophils and multiple lineage cytopenia. *Asxl1*$^{-/-}$ mice had a reduced hematopoietic stem cell (HSC) pool, and *Asxl1*$^{-/-}$ HSCs exhibited decreased hematopoietic repopulating capacity, with skewed cell differentiation favoring granulocytic lineage. *Asxl1*$^{+/-}$ mice also developed mild MDS-like disease, which could progress to MDS/myeloproliferative neoplasm, demonstrating a haploinsufficient effect of *Asxl1* in the pathogenesis of myeloid malignancies. *Asxl1* loss led to an increased apoptosis and mitosis in Lineage$^-$c-Kit$^+$ (Lin$^-$c-Kit$^+$) cells, consistent with human MDS. Furthermore, *Asxl1*$^{-/-}$ Lin$^-$c-Kit$^+$ cells exhibited decreased global levels of H3K27me3 and H3K4me3 and altered expression of genes regulating apoptosis (*Bcl2*, *Bcl2l12*, *Bcl2l13*). Collectively, we report a novel *ASXL1* murine model that recapitulates human myeloid malignancies, implying that Asxl1 functions as a tumor suppressor to maintain hematopoietic cell homeostasis. Future work is necessary to clarify the contribution of microenvironment to the hematopoietic phenotypes observed in the constitutional *Asxl1*$^{-/-}$ mice. (*Blood*. 2014;123(4):541-553)**

Introduction

Additional sex comb–like 1 (*ASXL1*) is a member of the Polycomb group of proteins, which are necessary for the maintenance of the stable repression of homeotic and other loci.[1-5] Recently, copious clinical studies showed that *ASXL1* is altered in multiple forms of myeloid malignancies, including myelodysplastic syndrome (MDS), myeloproliferative neoplasms (MPN), MDS/MPN (such as chronic myelomonocytic leukemia [CMML] and juvenile myelomonocytic leukemia [JMML]), and acute myeloid leukemia (AML).[6-12] Alterations in *ASXL1* are generally associated with signs of aggressiveness and poor prognosis in patients with CMML, MDS, myelofibrosis, and AML.[13-17] *ASXL1* alterations in myeloid malignancies have been reported as mutations and/or deletion, with the majority being frameshift and nonsense mutations,[6-12] resulting in C-terminal truncation of the protein upstream of the PHD finger. A recent study showed that truncated forms of the ASXL1 protein were undetectable in leukemia samples with *ASXL1* mutations, suggesting that these mutations are likely "bona fide loss-of-function" disease alleles.[18] However, it remains possible that truncated forms of ASXL1 resulting from *ASXL1* mutations in patients exert a gain-of-function and/or dominant-negative effect. Nevertheless, these clinical data suggest an important role of ASXL1 in the pathogenesis and/or transformation of myeloid malignancies. Therefore, it is important to elucidate the role ASXL1 plays in regulating normal hematopoiesis and pathogenesis of myeloid malignancies.

ASXL1 mutations in patients with myeloid malignancies are usually heterozygous,[17] suggesting a haploinsufficient effect of *ASXL1* in regulating hematopoietic stem/progenitor cell (HSC/HPC) functions and contributing to the development of myeloid malignancies. Intriguingly, de novo heterozygous mutations of *ASXL1* gene occur in Bohring-Opitz syndrome, a rare condition characterized by facial anomalies, multiple malformations, failure to thrive, severe intellectual disabilities, and early death.[19] These results suggest that somatic mutations of *ASXL1* lead to myeloid malignancies, whereas germline *ASXL1* mutations cause developmental phenotypes.

ASXL1 is mapped to chromosome 20q11, a region commonly involved in cancers.[1] Studies showed that ASXL1 regulates epigenetic marks and transcription through interaction with polycomb

Submitted May 2, 2013; accepted November 17, 2013. Prepublished online as *Blood* First Edition paper, November 19, 2013; DOI 10.1182/blood-2013-05-500272.

J.W., Z.L., and Y.H. contributed equally to this study.

The online version of this article contains a data supplement.

The publication costs of this article were defrayed in part by page charge payment. Therefore, and solely to indicate this fact, this article is hereby marked "advertisement" in accordance with 18 USC section 1734.

complex proteins and various transcription activators and repressors.[8,20,21] ASXL1 directly associates with BAP1 to form a PR-DUB complex, which deubiquitylates H2AK119.[18,20] However, a recent study showed that the impact of ASXL1 in leukemogenesis does not seem to be mediated by the DUB complex.[18] Importantly, ASXL1 interacts with components of the polycomb complex PRC2, which is involved in the deposition of H3K27me3 repressive marks.[18] Inhibition of ASXL1 function diminishes H3K27me3 histone marks, reinforcing the importance of ASXL1 in regulating the methylation of H3K27.[18] In addition, ASXL1 cooperates with HP1 to modulate the activity of LSD1,[4,21] a histone demethylase for H3K4 and H3K9.

Multiple in vitro studies in nonhematopoietic cells have suggested multiple activities for ASXL1, including physical cooperativity with HP1 and LSD1 to repress retinoic acid receptor activity and interaction with PPARγ to suppress lipogenesis.[4,21] Cooperative effects of *ASXL1* loss with other gene mutations in leukemogenesis have been suggested by a recent study showing that shRNA-mediated Asxl1-knockdown and NRasG12D overexpression triggered a more severe myeloid malignancy in vivo.[18] In an *Asxl1*-mutant mouse model, Fisher et al reported that *Asxl1* loss mildly perturbed myelopoiesis but did not trigger a hematologic malignancy.[22,23] The discrepancy between findings in human patients and the reported *Asxl1*-mutant model led us to wonder whether loss of function in *ASXL1* mutations is indeed causative or is a "driver" genetic event in the development and/or progression of myeloid malignancies. Likewise, the mechanism by which *ASXL1* mutations contribute to the pathogenesis of myeloid malignancies is of great importance in the field.

In the present study, we generated a murine model of *ASXL1* with complete knockout of *Asxl1*. We showed that $Asxl1^{-/-}$ mice had developmental abnormalities, including dwarfism, anophthalmia, and 80% embryonic lethality during late gestation. Approximately 78% of $Asxl1^{-/-}$ newborns died within 1 day after birth, and the remaining 22% of $Asxl1^{-/-}$ mice lived for 18 to 42 days. These surviving $Asxl1^{-/-}$ mice developed features of MDS. $Asxl1^{-/-}$ mice had a reduced HSC pool, and $Asxl1^{-/-}$ HSCs exhibited decreased hematopoietic repopulating capacity with skewed cell differentiation favoring granulocytic lineage. Importantly, $Asxl1^{+/-}$ mice also developed an MDS-like phenotype, indicating a haploinsufficient effect of *Asxl1* in the pathogenesis of myeloid malignancies. Moreover, *Asxl1* loss led to an increased apoptosis and mitosis in bone marrow (BM) cells and $Lin^{-}c\text{-}Kit^{+}$ HPCs, characteristics of human MDS. Therefore this *Asxl1* murine model recapitulates patients with MDS and provides a platform to investigate the cellular/molecular mechanisms by which *Asxl1* loss leads to the pathogenesis of myeloid malignancies. Our animal study was approved by Indiana University Institutional Review Board on Animal Care.

Material and methods

See supplemental Material and methods (available on the *Blood* Web site) for this information.

Results

Generation of *Asxl1:nlacZ/nGFP* knock-in and *Asxl1*-null murine models

Targeted *Asxl1*-null mice were generated by replacing part of exon 1 sequences of the *Asxl1* gene with *nlacZ/nGFP* (Figure 1A, supplemental Figure 1). The targeted allele results in transcription of *nlacZ* (*Asxl1:nlacZ/nGFP*) mRNA instead of *Asxl1* (disrupting endogenous ATG). Heterozygous *Asxl1:nlacZ/nGFP* ($Asxl1^{+/-}$) mice were interbred to obtain homozygous *Asxl1;nlacZ/nGFP* ($Asxl1^{-/-}$) mice. The mean litter size in $Asxl1^{+/-}$ intercrossing was smaller compared with wild-type (WT) intercrossing (7.4 ± 2.8 pups/litter vs 10.6 ± 2.0 pups/litter, $P < .01$). Genotypic analysis of 991 live births revealed that $Asxl1^{-/-}$ newborns were underrepresented (Figure 1B), suggesting embryonic lethality of ~80% of those embryos carrying both targeted alleles. This was confirmed by subsequent observation of dead $Asxl1^{-/-}$ embryos at embryonic day (E) 14.5 to 18.5 (supplemental Table 1). Moreover, ~78% of the $Asxl1^{-/-}$ newborn mice (52/67) died within 1 day after birth, and the remaining 22% of $Asxl1^{-/-}$ mice (15/67) survived for 18 to 42 days (Figure 1C). All surviving $Asxl1^{-/-}$ mice displayed dwarfism with profoundly lower body weight, albeit the size of $Asxl1^{+/-}$ mice was comparable with that of their WT littermates (Figure 1D-E). In addition, $Asxl1^{-/-}$ mice exhibited anophthalmia (supplemental Figure 2A-B). These results indicate that *Asxl1* deficiency leads to developmental abnormalities, including dwarfism and anophthalmia.

Analyses of *Asxl1* expression in BM cells

We then examined the expression of Asxl1 in BM cells of WT, $Asxl1^{+/-}$, or $Asxl1^{-/-}$ mice by Western blot analysis with an anti-Asxl1 antibody against Asxl1 N-terminus sequences. The full-length Asxl1 protein expression was not detected in $Asxl1^{-/-}$ and was significantly reduced in $Asxl1^{+/-}$ BM cells compared with WT cells (Figure 1F). To assess whether the mutant *Asxl1* allele generates aberrant splice variants of *Asxl1*, the expression of *Asxl1* mRNA in each genotype was analyzed with 4 different sets of primers (supplemental Table 2 and supplemental Figure 3). The *Asxl1* mRNA expression was not detectable in the BM cells of $Asxl1^{-/-}$ mice using any primer set (Figure 1G), indicating a complete deletion of *Asxl1* transcripts in $Asxl1^{-/-}$ mice. The *Asxl1* mRNA expression in $Asxl1^{+/-}$ BM cells was decreased by 35% to 50% compared with that in WT cells (Figure 1G). The levels of *Asxl2* and *Asxl3* mRNA expression were comparable in BM cells from each genotype of mice (data not shown).

Loss of *Asxl1* leads to MDS-like disease

We first examined whether loss of *Asxl1* resulted in manifestations of myeloid malignancies in the surviving young $Asxl1^{-/-}$ mice (n = 9, 18-42 days old). May-Giemsa–stained peripheral blood (PB) smears prepared from these young $Asxl1^{-/-}$ mice showed dysplastic features, including hypersegmented neutrophils, hyposegmented (bilobed) neutrophils (supplemental Figure 4) with fine nuclear bridging consistent with pseudo–Pelger-Huët anomaly, an increased number of polychromatophilic red blood cells (RBCs), and Howell-Jolly body in erythrocytes (Figure 2A), whereas blasts were rare. PB counts of these young $Asxl1^{-/-}$ mice revealed multiple cytopenias consistent with myelodysplasia and ineffective hematopoiesis. Leukocytopenia was observed in 3 of the 9, thrombocytopenia was detected in 6 of the 9, and anemia was evident in 3 of the 9 $Asxl1^{-/-}$ mice (Figure 2B).

The BM of these young $Asxl1^{-/-}$ mice exhibited normo- or hypercellularity as determined by cellularity/femur/body weight (supplemental Figure 5A-B). Morphologic examination of the BM of these $Asxl1^{-/-}$ mice revealed myeloid hyperplasia and relative erythroid hypoplasia with smaller erythroid islands compared with WT (Figure 2Ca-d). In addition, megakaryocytes in $Asxl1^{-/-}$ marrow

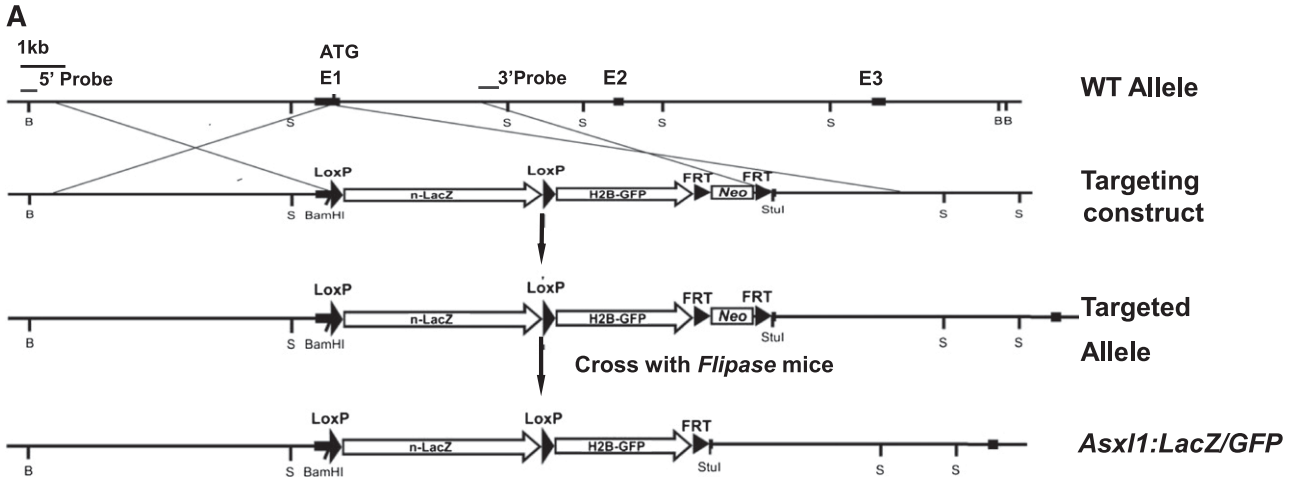

B

Genotype distribution among live births of *Asxl1*$^{+/-}$ intercross					
Parental *Asxl1* genotype	Total offspring	*Asxl1* genotype			P value
		+/+ N (%)	+/- N (%)	-/- N (%)	
+/- cross +/-	991	317 (32.0)	607 (61.2)	67 (6.8)	<0.001

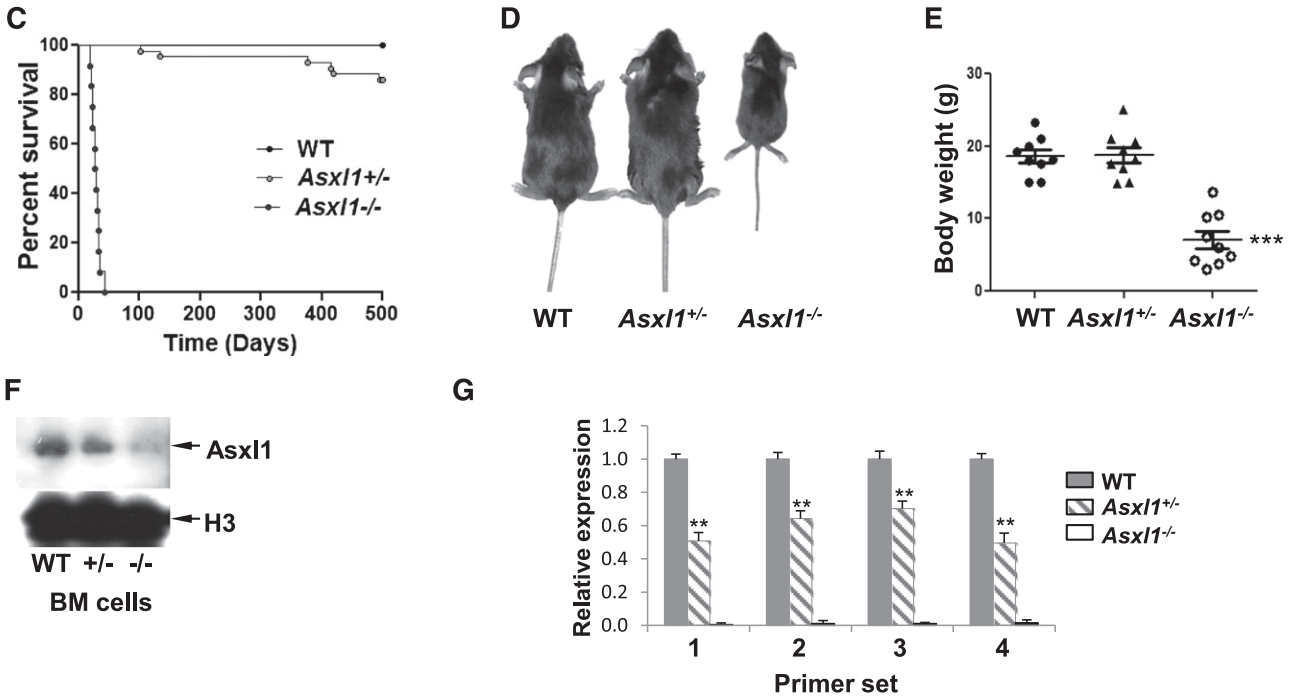

Figure 1. Generation of *Asxl1:nlacZ/nGFP* knock-in mice. (A) An *nlacZ/nGFP-FRTNeoFRT* cassette was introduced 6 bp upstream of the *Asxl1* start codon. Rectangular black bars indicate exons. S, *StuI*. (B) Genotype distribution among live births of *Asxl1*$^{+/-}$ intercross. *Asxl1*$^{-/-}$ mice are underrepresented. *P* values are compared with normal Mendelian distribution (25%, 50%, 25%) using a χ^2 test. (C) Kaplan-Meier curve representing the percent survival of *Asxl1*$^{-/-}$ (n = 12), *Asxl1*$^{+/-}$ (n = 42), and WT (n = 42) mice vs age in days. (D) The gross appearance of an *Asxl1*$^{-/-}$ mouse compared with WT and *Asxl1*$^{+/-}$ littermates (4 weeks old). (E) Body weight of WT, *Asxl1*$^{+/-}$, and *Asxl1*$^{-/-}$ mice (3-6 weeks old, 9 mice/genotype; ***$P < .001$). (F) Western blot shows the reduced and deletion of Asxl1 expression in BM cells of representative *Asxl1*$^{+/-}$ and *Asxl1*$^{-/-}$ mice, respectively, compared with WT. (G) Analyses of *Asxl1* mRNA expression levels in BM cells of WT (n = 4), *Asxl1*$^{+/-}$ (n = 5), and *Asxl1*$^{-/-}$ (n = 5) mice by qPCR with 4 different pairs of primers. The relative *Asxl1* mRNA expression was determined by using β-actin as an internal calibrator and reported as relative expression units to the respective *Asxl1* expression with each primer pair in WT mice. **$P < .01$, ***$P < .001$

were significantly smaller with hypolobated nuclei compared with megakaryocytes with multilobated nuclei in WT BM. Interestingly, spleen, but not liver, of these *Asxl1*$^{-/-}$ mice were of dramatically lower volume and weight (hyposplenia) than those of their WT and *Asxl1*$^{+/-}$ littermates (supplemental Figure 5C-E). The histology of the *Asxl1*$^{-/-}$ spleen revealed features of spleen atrophy, with

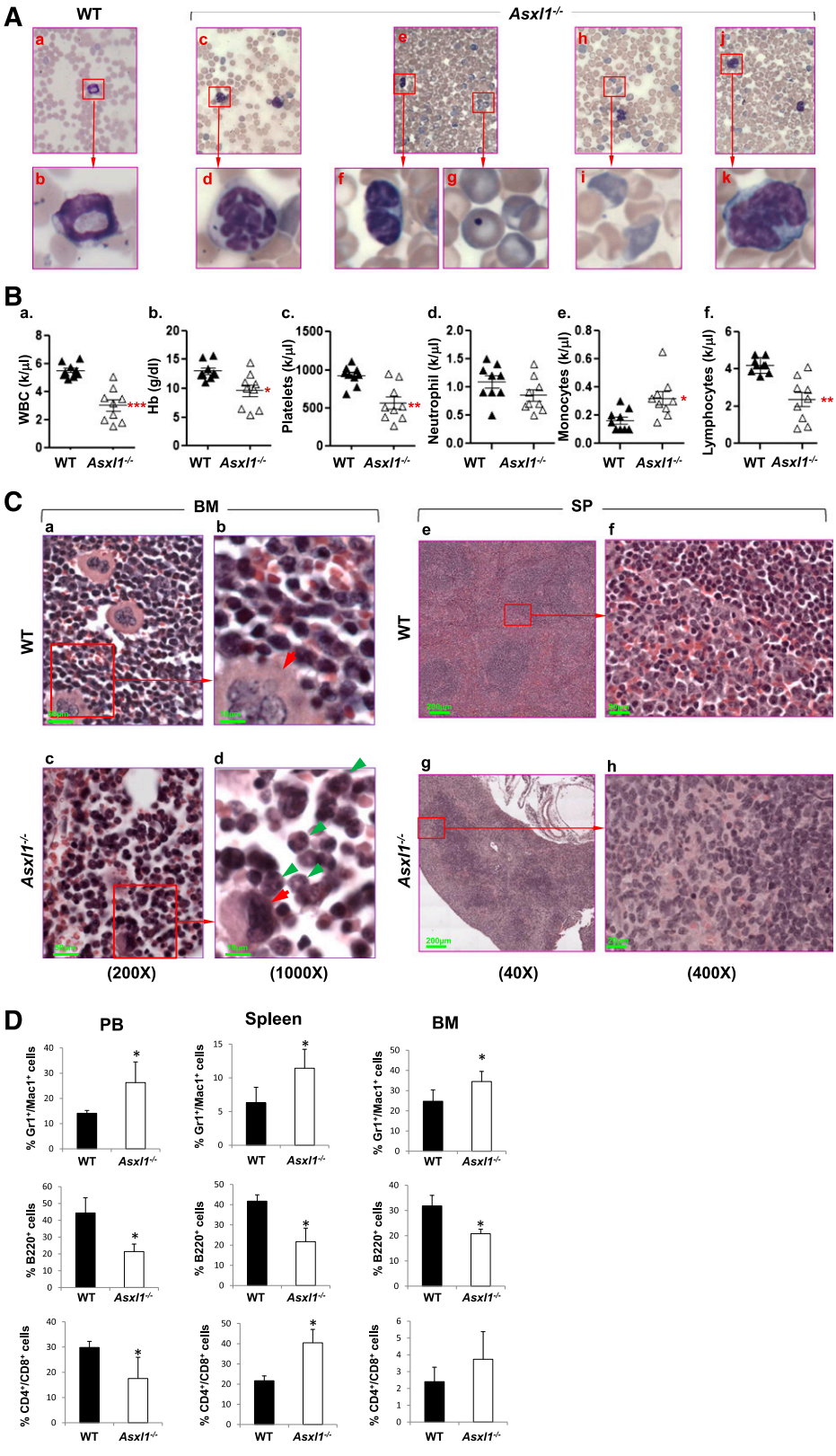

Figure 2. Loss of *Asxl1* leads to MDS-like disease. (A) May-Giemsa–stained PB smears prepared from representative WT (a-b) and *Asxl1*$^{-/-}$ (c-k) mice are shown. The PB smear of *Asxl1*$^{-/-}$ mice showed dysplastic features including hypersegmented neutrophils (c-d), bilobed and hyposegmented neutrophils (e-f) consistent with pseudo–Pelger-Huët anomaly, as well as an increased number of polychromatophilic RBCs (h-i), and Howell-Jolly body in erythrocytes (e,g). The PB smear of representative *Asxl1*$^{-/-}$ mice showed monocytosis (j-k). (B) Parameters of PB were summarized from WT (n = 9) and *Asxl1*$^{-/-}$ (n = 9) mice of 3 to 6 weeks of age: WBC counts (a), Hb (b), platelets (c), neutrophils (d), monocytes (e), and lymphocytes (f). *$P < .05$, **$P < .01$. (C) Hematoxylin and eosin staining of paraffin-embedded sections of femurs (a-d) and spleen (e-h) from representative WT and *Asxl1*$^{-/-}$ mice (4 weeks old). BM: original magnification ×20 in (a) and (c), and original magnification ×100 in (b) and (d). Red arrows indicate megakaryocytes, and green arrows indicate myeloid cells. SP: original magnification ×4 in (e) and (g), and original magnification ×40 in (g) and (h). (D) Quantitation of the Gr1$^+$/Mac1$^+$, B220$^+$, and CD4$^+$/CD8$^+$ cell populations. Percentage in PB, spleen, and BM cells of WT and *Asxl1*$^{-/-}$ mice (3-5 weeks old). Data are presented as mean ± SD from 4 sets of WT and *Asxl1*$^{-/-}$ littermates. *$P < .05$.

dramatically reduced cellularity of the red pulp (Figure 2Ce-h). Lymphoid aggregates in the white pulp (disrupted architecture) of the *Asxl1*$^{-/-}$ spleen were also smaller than those of WT spleen. Consistently, flow cytometric analyses of *Asxl1*$^{-/-}$ PB, BM, and spleen cells revealed an increased proportion of granulocytic/monocytic cells (Gr-1$^+$/Mac1$^+$) but a decreased proportion of B220$^+$

B cells (Figure 2D and supplemental Figure 6). The proportion of $CD4^+$ and $CD8^+$ T cells was also increased in the spleen, which might be relative to the decreased B-cell population (Figure 2D and supplemental Figure 6). Collectively, these data show that *Asxl1* deletion leads to a disease phenotype resembling clinical manifestations of MDS in human.

Haploinsufficiency of *Asxl1* is sufficient for the development of MDS-like disease and MDS/MPN

The majority of the *ASXL1* mutations in patients with myeloid malignancies are heterozygous.[6-12] We next examined whether haploinsufficiency of *Asxl1* is sufficient for the development of myeloid malignancies by analyzing a cohort of 10 young (3-6 weeks old) and 18 adult (6-12 months old) $Asxl1^{+/-}$ mice. May-Giemsa–stained PB smears prepared from each of the $Asxl1^{+/-}$ mice showed dysplastic features, including hypersegmented neutrophils, hyposegmented (bilobed) neutrophils consistent with pseudo–Pelger-Huët anomaly, frequent apoptotic neutrophils, hypogranulated neutrophils, and an increased number of polychromatophilic RBCs (Figure 3A). Interestingly, adult $Asxl1^{+/-}$ mice exhibited more severe dysplasia of myeloid lineage than young $Asxl1^{+/-}$ mice, indicating disease progression. The age-dependent disease progression in $Asxl1^{+/-}$ mice was also substantiated by the PB counts and histologic and flow cytometric analyses. The adult $Asxl1^{+/-}$ mice displayed a higher frequency of anemia and thrombocytopenia than did the young $Asxl1^{+/-}$ mice. In addition, white blood cell (WBC) counts of adult $Asxl1^{+/-}$ mice were more heterogeneous, with many mice showing leukopenia, including neutropenia, and some mice displaying leukocytosis and monocytosis (Figure 3B). Absolute monocytosis/neutrophilia was identified in 4 of the 18 adult $Asxl1^{+/-}$ mice (22%) but in none of the young $Asxl1^{+/-}$ mice (Figure 3B). The presence of anemia, thrombocytopenia, leukocytosis, absolute monocytosis/neutrophilia, and dysplasia is consistent with human MDS/MPN, especially CMML. Histologic analysis of spleen and liver sections of the adult $Asxl1^{+/-}$ mice showed disrupted splenic architecture, with an increased proportion of myeloid cells, and perivascular myeloid cell infiltration in the liver (Figure 3C). BM histologic sections of adult $Asxl1^{+/-}$ mice revealed an increase in the proportion of myeloid cells and relatively decreased erythroid islands (Figure 3D). Compared with their WT counterparts, adult $Asxl1^{+/-}$ mice showed an increased myeloid/erythroid ratio (WT = 2.6 ± 0.3, $Asxl1^{+/-}$ with MDS-like disease = 4.2 ± 1.2; $P < .05$ and $Asxl1^{+/-}$ with MDS/MPN = 6.5 ± 2.1, $P < .01$; n = 4-5). Dysplastic myeloid cells were also frequently seen in $Asxl1^{+/-}$ BM (Figure 3D). Flow cytometric analysis confirmed the increased granulocytic/monocytic ($Gr\text{-}1^+/Mac\text{-}1^+$) and decreased $B220^+$ B-cell populations in the BM and spleen of adult $Asxl1^{+/-}$ mice, whereas the proportions of $CD4^+/CD8^+$ cell populations in the BM and spleen were comparable (Figure 3E, supplemental Figure 7). These data suggest that haploinsufficiency of *Asxl1* is sufficient to cause MDS-like disease and/or MDS/MPN in mice.

Notably, one $Asxl1^{+/-}$ mouse (B8) developed overt disease and became moribund at 16 months of age. In addition to elevated WBC counts and anemia (supplemental Table 3), necropsy revealed splenomegaly and a large mass in the uterus (supplemental Figure 8A). Flow cytometric analysis indicated that this mass was composed of $Gr\text{-}1^+/Mac1^+$ cells, suggesting myeloid sarcoma (supplemental Figure 8B-C). A tumor transfer assay showed that transferring 1×10^6 spleen cells from this aged, end-disease stage $Asxl1^{+/-}$ mouse successfully caused neutrophilia/monocytosis and splenomegaly in sublethally irradiated WT recipients, verifying the malignant nature of the cells from the moribund $Asxl1^{+/-}$ mouse (supplemental Figure 8D). On the basis of the Bethesda proposals for classifying nonlymphoid hematopoietic neoplasms in mice,[24] the pathology in this moribund $Asxl1^{+/-}$ mouse met the criteria for myeloid leukemia with maturation (neoplastic cells showed some maturation, more than 20% immature forms/blasts in the BM, supplemental Figure 8E-F). Collectively, heterozygous deletion of *Asxl1* leads to the development of MDS-like disease in mice, some of which could progress/transform to MDS/MPN and myeloid leukemia (Table 1, supplemental Table 3). Approximately 14% of the $Asxl1^{+/-}$ mice (up to 16 months) became moribund or died as a result of severe myeloid malignancies (Figure 1C). These findings are significantly clinically relevant because *ASXL1* mutations are associated with a more aggressive clinical course in MDS/CMML patients and have a high risk to progress to leukemia.[13-17]

Asxl1 loss leads to increased apoptotic and mitotic cells in BM

Increased apoptosis and cell proliferation are characteristic features of MDS.[25] We next examined whether *Asxl1* loss affected the apoptosis and mitosis of BM cells. May-Giemsa–stained BM cell cytospin preparations revealed a higher proportion of apoptotic and mitotic cells in $Asxl1^{+/-}$ and $Asxl1^{-/-}$ BM compared with WT BM, in which apoptotic and mitotic cells were rarely seen (supplemental Figure 9A). When BM cells were evaluated for apoptosis by Annexin V/7-AAD staining after 18-hour starvation, starvation-induced apoptosis was significantly greater in $Asxl1^{+/-}$ and $Asxl1^{-/-}$ BM cells compared with WT controls (supplemental Figure 9B-C). In addition, when freshly isolated BM $Lin^-c\text{-}Kit^+$ cells were analyzed for apoptosis (Figure 4A-B) and cytokine cocktail–stimulated $Lin^-c\text{-}Kit^+$ cells were analyzed for cell-cycle profiling (Figure 4C), a significantly higher percentage of apoptotic cells and cells of S/G2/M phases were observed in $Asxl1^{-/-}$ $Lin^-c\text{-}Kit^+$ cells than that in WT cells. $Asxl1^{+/-}$ $Lin^-c\text{-}Kit^+$ cells also contained a higher proportion of apoptotic cells than did WT controls (Figure 4A-B). Furthermore, examination of May-Giemsa–stained cytospin preparations of colonies derived from $Asxl1^{+/-}$ or $Asxl1^{-/-}$ BM cells (with mSCF, mIL-3, EPO, and IL-6 for 8 days) revealed dramatically increased proportions of mitotic cells compared with WT BM cell–derived colonies (Figure 4D-E). A significantly higher proportion of mitotic cells was also noted in $Asxl1^{-/-}$ BM cell–derived colonies than in $Asxl1^{+/-}$ BM cell–derived colonies. These data indicate that *Asxl1* loss in mice resulted in increased apoptosis and mitosis of BM cells, consistent with cellular phenotypes of human MDS.

Altered HSC and myeloid progenitor populations in *Asxl1*$^{-/-}$ mice

To determine whether deleting *Asxl1* affects the HSC/HPC pool in vivo, we analyzed the $Lin^-Sca1^+c\text{-}Kit^+$ (LSK) and $Lin^-Sca1^-c\text{-}Kit^+$ (LK) cell populations in the BM of young WT, $Asxl1^{+/-}$, and $Asxl1^{-/-}$ mice (3-6 weeks old). The proportion of LSK cells, but not LK cells, was significantly decreased in young $Asxl1^{-/-}$ mice compared with WT controls (Figure 5A-C). When the myeloid progenitor populations were analyzed within the LK populations, the percentage of granulocyte-macrophage progenitor (GMP) population was higher, whereas megakaryocyte-erythroid progenitor (MEP) population was lower in the BM of $Asxl1^{-/-}$ mice compared with that of WT and $Asxl1^{+/-}$ mice (Figure 5D-E). Consistently, colony assays revealed a moderate decrease in colony-forming unit (CFU)-C and burst-forming unit–E frequency of $Asxl1^{-/-}$ BM cells compared with WT

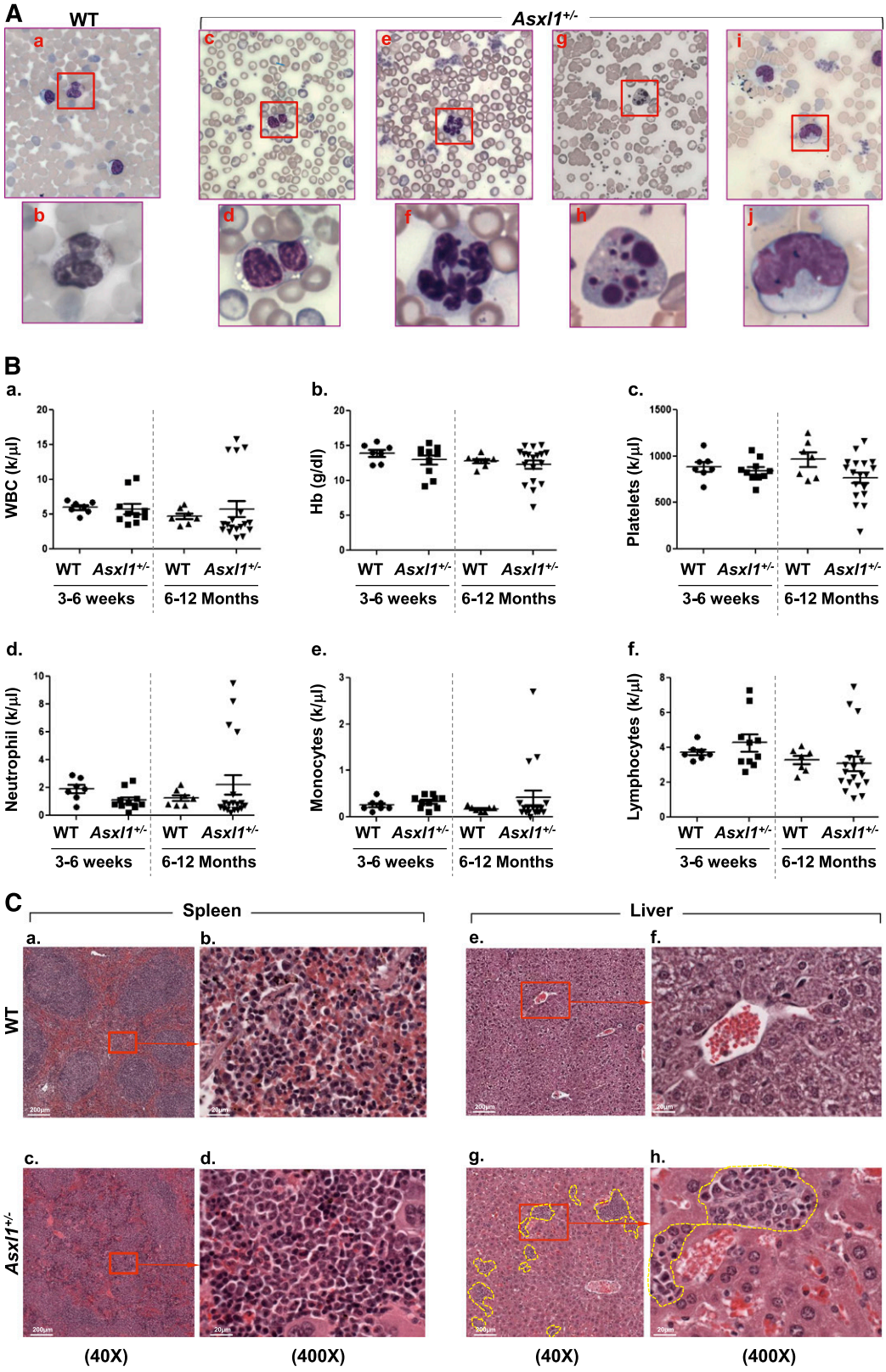

Figure 3. Haploinsufficiency of *Asxl1* is sufficient for the development of MDS-like disease and MDS/MPN in mice. (A) May-Giemsa–stained PB smears prepared from representative adult WT (a-b) and *Asxl1*$^{+/-}$ (c-j) mice (6-12 months old) are shown. The PB smear of *Asxl1*$^{+/-}$ mice showed dysplastic features including bilobed and hyposegmented neutrophils with clumping chromatin consistent with pseudo–Pelger-Huët anomaly (c-d), hypersegmented neutrophils (e-f), and apoptotic neutrophils (g-h). The PB smear of representative *Asxl1*$^{+/-}$ mice showed monocytosis (i-j). (B) Parameters of PB were summarized from young WT (n = 7) and *Asxl1*$^{+/-}$ (3-6 weeks old,

Figure 3. (Continued).

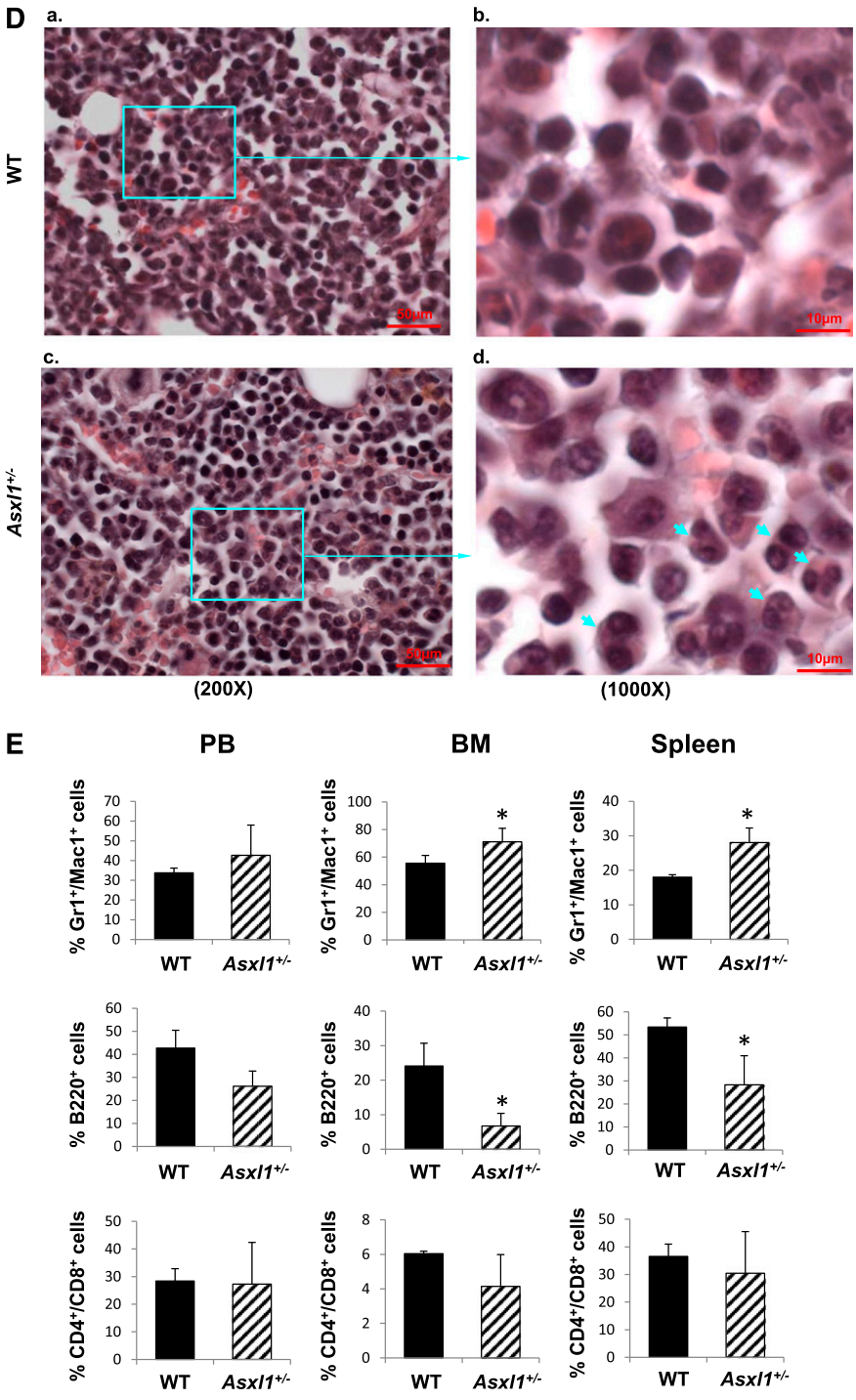

controls (Figure 5F), presumably because of a decreased frequency and increased apoptosis of HSC/HPCs. These data suggest that *Asxl1* deletion decreases the HSC pools and alters the GMP and MEP populations in young mice.

Interestingly, when the LSK and LK cell populations in the BM of adult $Asxl1^{+/-}$ mice were examined, the proportion of both LSK and LK cells was significantly greater in adult $Asxl1^{+/-}$ mice with MDS/MPN but was smaller in adult $Asxl1^{+/-}$ mice with

Figure 3 (continued) n = 10) and aged WT (n = 7) and adult $Asxl1^{+/-}$ (6-12 months old, n = 18) mice: WBC counts (a), Hb (b), platelets (c), neutrophils (d), monocytes (e), and lymphocytes (f). (C-D) Hematoxylin and eosin staining of paraffin-embedded sections of spleen (C, right), liver (C, left), and femurs (D), from representative aged WT and $Asxl1^{+/-}$ mice. Yellow lines represent areas containing infiltrating myeloid cells (Cg-h). Blue arrows indicate dysplastic cells (Dd). Spleen and liver: original magnification ×4 in (a), (c), (e), and (g); and original magnification ×40 in (b), (d), (f), and (h). BM: original magnification ×20 in (a) and (c), and original magnification ×100 in (b) and (d). (E) Quantitation of the percentage of $Gr1^+/Mac1^+$, $B220^+$, and $CD4^+/CD8^+$ cell populations in PB, spleen, and BM of WT and $Asxl1^{+/-}$ mice (6-12 months old). Data are presented as mean ± SD from 5 sets of WT and $Asxl1^{+/-}$ littermates. *$P < .05$.

Table 1. Diagnosis and subclassification of the myeloid malignancies developed in 18 adult *Asxl1*$^{+/-}$ mice

Age (days)	Frequency	Necropsy and other findings	Blood counts	BM Blasts (%)	Dysplastic Neutrophil	Transplantability	Diagnosis and subclassification
131~ 495	72.2% (13/18)	Liver and spleen with myeloid infiltration	WBC → ↓ NE → MO → Plt → ↓ RBC → ↓	<20%	Yes	No (n=2)	MDS or MDS-like
102 ~ 495	22.2% (4/18)	Splenomegaly (1/4), liver and spleen with myeloid infiltration	WBC ↑ NE ↑ MO → ↑ Plt → ↓ RBC → ↓	<20%	Yes	No (n=2)	MDS/MPN
495	5.6% (1/18)	Hepatosplenomegaly mass in uterus (myeloid sarcoma)	WBC ↑ NE ↑ MO ↑ Plt → RBC ↓	>20%	Yes	Yes* (n=1)	Myeloid leukemia with maturation

*See supplemental Figure 8D.

MDS compared with age-matched WT controls (supplemental Figure 10A-C). Moreover, the GMP frequency was dramatically increased and MEP frequency significantly decreased in adult *Asxl1*$^{+/-}$ mice with MDS/MPN but not in adult *Asxl1*$^{+/-}$ mice with MDS (supplemental Figure 10D-E). Consistently, the BM and spleen cells of adult *Asxl1*$^{+/-}$ mice with MDS/MPN contained higher frequencies, and adult *Asxl1*$^{+/-}$ mice with MDS had lower frequencies, of CFU-C compared with WT controls (supplemental Figure 10F-G). These data suggest that *Asxl1* haploinsufficiency differentially alters HSC/HPC pools as animals develop different spectrum of myeloid malignancies.

Asxl1 loss impairs hematopoietic repopulating capacity

We next performed a competitive repopulation assay to determine whether deleting *Asxl1* affects the cell fates of HSCs in vivo. When PB was determined for donor chimerism 1, 2, 4, 6, or 10 months after transplantation, the CD45.2 chimerisms remained ~50% in mice receiving WT BM cells, whereas a steady decline in the CD45.2 chimerism was observed in mice receiving *Asxl1*$^{+/-}$ or *Asxl1*$^{-/-}$ BM cells, with a significantly lower CD45.2 chimerism in mice receiving *Asxl1*$^{-/-}$ BM cells (Figure 6A). At month 10, the CD45.2 chimerism decreased to less than 10% in the PB of mice receiving *Asxl1*$^{-/-}$ BM cells. Consistent with PB, the CD45.2 chimerism was significantly lower in the BM of mice receiving *Asxl1*$^{-/-}$ or *Asxl1*$^{+/-}$ BM cells than in the mice receiving WT BM cells (Figure 6B). Interestingly, *Asxl1*$^{-/-}$ BM cells contributed to a greater proportion of Gr-1^{+}/Mac1^{+} granulocytic/monocytic cells, a smaller proportion of B220^{+} B cells, and significantly smaller proportions of LSK and LK HSC/HPCs in the recipient BM compared with the WT controls. In addition, serial transplantation showed a stable BM CD45.2 chimerism (range 42%-52%) in WT BM transplants, whereas BM CD45.2 chimerism decreased upon each round of *Asxl1*$^{+/-}$ or *Asxl1*$^{-/-}$ BM transplantation, with a sharper decline in *Asxl1*$^{-/-}$ BM transplants (Figure 6C). These data suggest that *Asxl1* deletion/haploinsufficiency impairs the long-term repopulating capacity and self-renewal of HSCs and likely confers a skewed differentiation toward granulocytic/monocytic lineage in vivo.

Deletion of *Asxl1* altered expression of genes implicated in apoptosis regulation and reduced global levels of H3K27me3 and H3K4me3 in Lin^{-}c-Kit^{+} cells

The Polycomb group of proteins maintains the "off state" of the clustered homeotic box (*Hox*) genes, and Asxl1 is a member of the Polycomb group of proteins.[26] We then determined whether deletion of *Asxl1* leads to altered expression of *HoxA* genes (*HoxA5/7/9/10*) in Lin^{-}c-Kit^{+} cells by quantitative polymerase chain reaction (qPCR). The expression of each of these *HoxA* genes was significantly higher in *Asxl1*$^{-/-}$ BM Lin^{-}c-Kit^{+} cells than in WT Lin^{-}c-Kit^{+} cells (Figure 7A). *Asxl1*$^{-/-}$ Lin^{-}c-Kit^{+} cells are characterized by increased apoptosis. We therefore examined the expression of several genes implicated in apoptosis regulation, including *Bcl2*, *Bcl2l12*, and *Bcl2l13*. *Bcl2l13* (an apoptosis facilitator) was upregulated, whereas *Bcl2* and *Bcl2l12* (pro-apoptotic genes) were downregulated in *Asxl1*$^{-/-}$ Lin^{-}c-Kit^{+} cells (Figure 7A), which might contribute to the increased apoptosis of *Asxl1*$^{-/-}$ Lin^{-}c-Kit^{+} cells.

ASXL1 knockdown has recently been shown to significantly reduce global H3K27me3 levels in myeloid cells.[18] We next examined whether deleting *Asxl1* altered the global H3 methylation states in Lin^{-}c-Kit^{+} cells. Western blot analysis with nuclear extracts of Lin^{-}c-Kit^{+} cells showed decreased levels of global H3K4me3 and H3K27me3 in *Asxl1*$^{-/-}$ Lin^{-}c-Kit^{+} cells compared with WT and *Asxl1*$^{+/-}$ Lin^{-}c-Kit^{+} cells (Figure 7B). These results indicate that Asxl1 is required to maintain H3 methylation states in HSC/HPCs.

Discussion

Despite the clinical importance of *ASXL1* mutations in the myeloid malignancies, the cellular and molecular mechanisms underpinning the *ASXL1* loss–mediated pathogenesis of myeloid malignancies remains largely unknown. In the present study, using our newly generated *Asxl1* knockout murine model, we made several important observations. First, *Asxl1* deletion in mice led to developmental abnormalities including dwarfism and

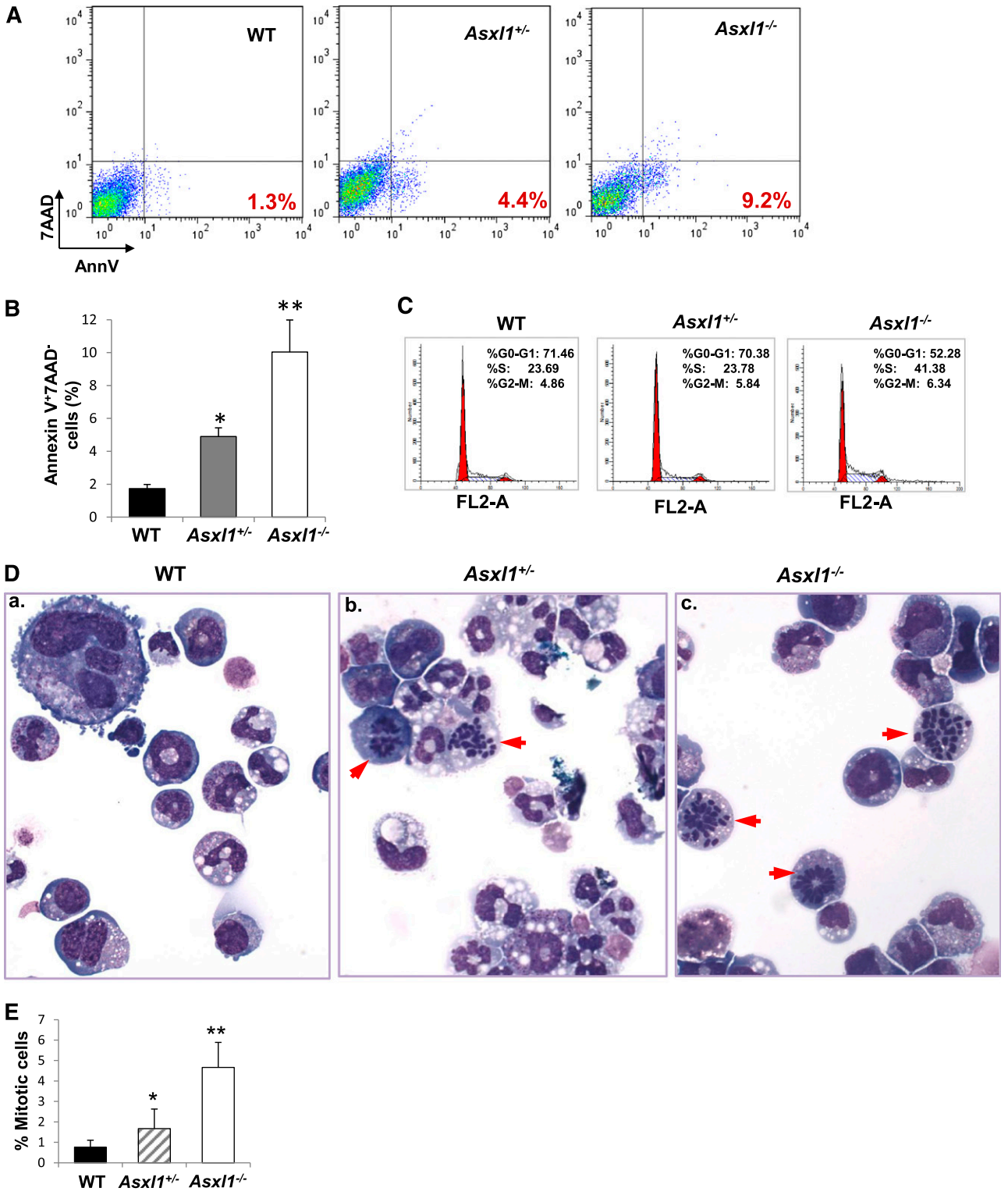

Figure 4. *Asxl1* loss leads to increased apoptotic and mitotic cells in BM Lin$^-$c-Kit$^+$ cells. (A) Flow cytometric analysis of freshly isolated Lin$^-$c-Kit$^+$ cells from the BM of representative WT, *Asxl1*$^{+/-}$, and *Asxl1*$^{-/-}$ littermates (5 weeks old) after Annexin V/7-AAD staining. (B) Quantitation of the subgroup of apoptotic cell population that is Annexin V$^+$/7-AAD$^-$. Data are presented as mean ± SD from 3 sets of WT, *Asxl1*$^{+/-}$, and *Asxl1*$^{-/-}$ mice (4-5 weeks old). (C) Cell cycle analysis of Lin$^-$c-Kit$^+$ cells from representative WT, *Asxl1*$^{+/-}$, and *Asxl1*$^{-/-}$ littermates are shown (5 weeks old). Similar results were obtained using another set of *Asxl1* littermates of mice (4 weeks old). (D-E) Representative images of May-Giemsa–stained cytospin preparations of cells from WT, *Asxl1*$^{+/-}$, or *Asxl1*$^{-/-}$ BM cell–derived colonies showing an increased proportion of mitotic cells (red arrowheads, D). The quantitation of the percent of mitotic cells is shown by performing a 500-cell count of at least 10 colonies from each genotype (E). Representative data from 2 separate experiments are shown as mean ± SD. *$P < .05$, **$P < .01$.

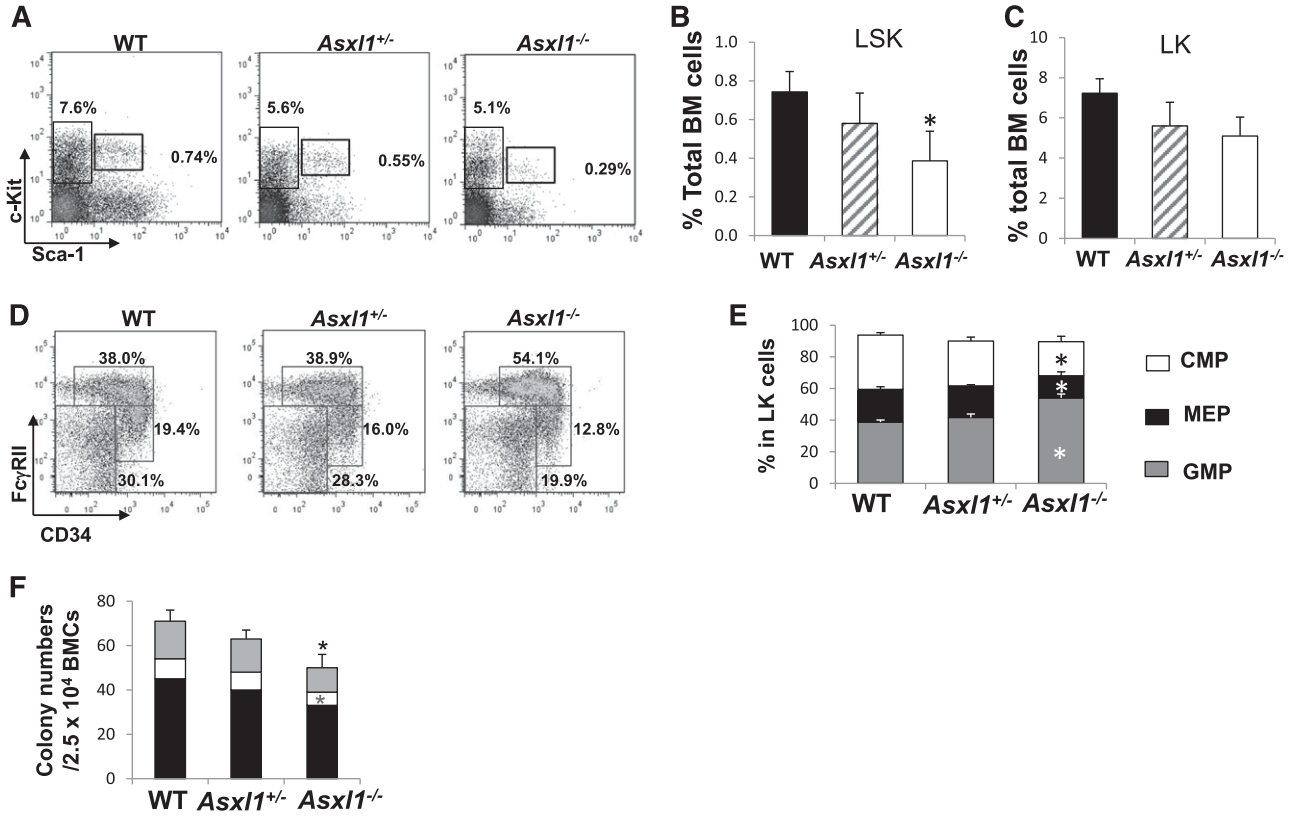

Figure 5. Altered HSC and myeloid progenitor cell populations in *Asxl1*$^{-/-}$ mice. (A) Flow cytometric analysis of LSK and LK compartments in the BM of representative young WT, *Asxl1*$^{+/-}$, and *Asxl1*$^{-/-}$ mice (4 weeks old). (B-C) Quantitation of the percent of LSK (B) and LK (C) cells in the total BM cells of each genotype of mice (mean ± SD, 4-5 mice/genotype, 3-6 weeks old, *$P < .05$). (D) Flow cytometric analysis of CMP, GMP, and MEP populations in the BM LK cell population of WT, *Asxl1*$^{+/-}$, and *Asxl1*$^{-/-}$ mice are shown. (E) Quantitative analysis of CMP, GMP, and MEP populations in the LK cell population (4-5 mice/group, 3-6 weeks old, *$P < .05$). (F) BM progenitor assay. CFU numbers were assessed in semisolid media in the presence of mSCF, mIL-3, IL-6, and EPO. Data are presented as mean ± SEM from 4 to 5 mice per genotype. Black bars represent CFU-GM (granulocytes/macrophages), open bars represent BFU-E (burst forming unit-erythrocyte), and gray bars represent CFU-Mix (mixed colonies of GM, E, and megakaryocytic cells). *$P < .05$.

anophthalmia. Second, *Asxl1*$^{-/-}$ mice developed a phenotype resembling many characteristics of MDS. Third, deletion of *Asxl1* reduces the HSC pool and decreases HSC hematopoietic repopulating capacity in vivo, which is associated with increased apoptosis and mitosis. Fourth, *Asxl1*$^{+/-}$ mice also developed a mild MDS-like disease, which could progress to MDS/MPN, demonstrating a haploinsufficient effect of *Asxl1* in the pathogenesis of myeloid malignancies.

De novo mutations in the *ASXL1* gene have been shown to account for approximate 50% cases of Bohring-Opitz syndrome, which is a rare disease characterized by facial anomalies, multiple malformations, failure to thrive, and severe intellectual disabilities.[19] This severe condition often leads to death at an early age, preventing knowledge of whether susceptibility to myeloid malignancies might result from *ASXL1* germ-line mutations. Fisher et al showed that *Asxl1*-mutant mice exhibited alterations of the axial skeleton.[23] In this study, we showed that *Asxl1*-deletion caused multiple developmental defects in mice including dwarfism and anophthalmia. The mechanisms by which *Asxl1* deletion causes developmental defects needs to be elucidated.

The majority of myeloid malignancy patients with *ASXL1* mutations retain a WT copy and a mutant allele of *ASXL1*, which leads to nonsense/frameshift, suggesting loss of function.[6-12] Therefore *ASXL1* has been speculated to be a putative tumor suppressor gene that is strongly implicated in the pathogenesis of myeloid malignancies. Consistent with the clinical genetic characteristics, haploinsufficient loss of *Asxl1* in mice leads to the development of MDS-like disease. These data provide persuasive functional evidence that haploinsufficiency of *Asxl1* is sufficient to cause MDS-like disease in vivo. In addition, a subset of *Asxl1*$^{+/-}$ mice progress to MDS/MPN as they age, displaying neutrophilia and/or monocytosis, and an increased number of granulocytic/monocytic cells in the BM, suggesting that *ASXL1* loss can lead to myelomonocytic expansion. This is consistent with the observations that *ASXL1* mutations are common in CMML, which is classified as a MDS/MPN.[6-12] Clonal dominance is a defining feature of MDS. Concomitant mutations have been frequently found in myeloid malignancy patients with *ASXL1* mutations. It is possible that *Asxl1*$^{+/-}$ mice could acquire mutations in critical genes, promoting the clonal dominance over time. Indeed, MDS in 1 aged *Asxl1*$^{+/-}$ mouse progressed to myeloid leukemia, which was transferable into sublethally irradiated naïve WT recipient mice. Multiple clinical studies have shown that mutations in *ASXL1* are associated with signs of aggressiveness and poor prognosis in patients with CMML, MDS, myelofibrosis, and AML.[13-17] In MDS and CMML, *ASXL1* mutations are frequently present in chronic phases and precede transformation.[27] Data obtained from the animal model are consistent with these clinical observations.

Increased apoptosis and mitosis of hematopoietic precursors are characteristic cellular features of human MDS.[25] Bouscary et al reported that the proliferation of dysplastic clones is likely accompanied by a significant increase in apoptosis.[28] We consistently

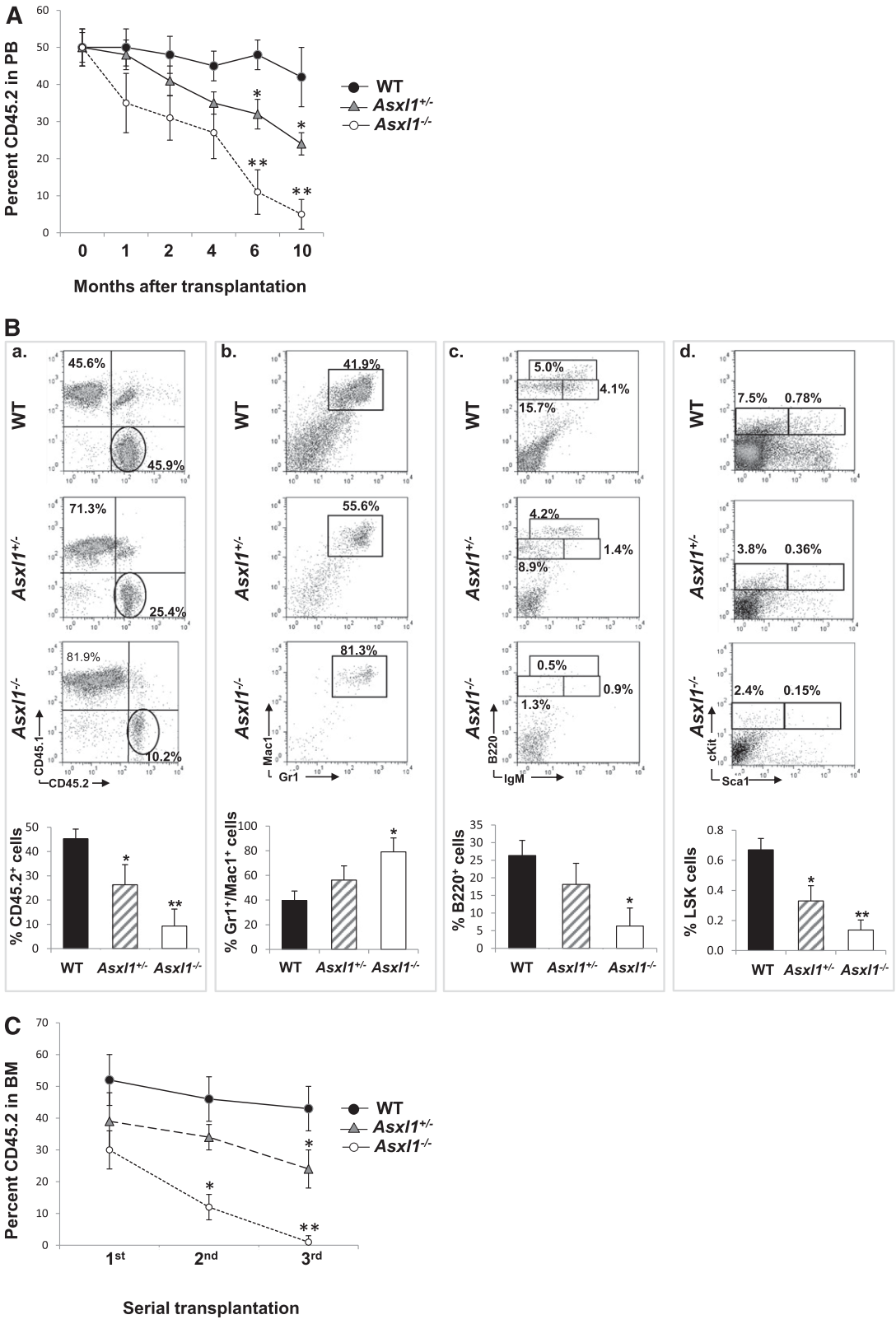

Figure 6. Asxl1 loss impaired the hematopoietic repopulation capacity of HSCs. CD45.2$^+$ BM cells from young WT, *Asxl1*$^{+/-}$, or *Asxl1*$^{-/-}$ mice were mixed with CD45.1$^+$ competitor cells at a ratio of 1:1 (1×10^6 cells each) and transplanted into lethally irradiated F1 recipients. (A) The kinetics of CD45.2 chimerism in the PB of mice receiving WT, *Asxl1*$^{+/-}$, or *Asxl1*$^{-/-}$ BM cells are shown (mean ± SD of 3-7 animals). (B) Flow cytometric analysis of BM cells from representative mice receiving WT, *Asxl1*$^{+/-}$, or *Asxl1*$^{-/-}$ BM cells 10 months after transplantation using indicated antibody combinations. The percent CD45.2$^+$ cells as well as Gr1$^+$/Mac1$^+$, B220$^+$, and LSK distribution within the CD45.2$^+$ cells in the BM of each group of recipient mice is shown (mean ± SD of 3-5 animals). (C) Serial transplantations were performed as described in supplemental Material and methods. The percent CD45.2 chimerism in the BM of recipient mice 4 months after each round of transplantation is show as mean ± SEM. *$P < .05$, **$P < .01$.

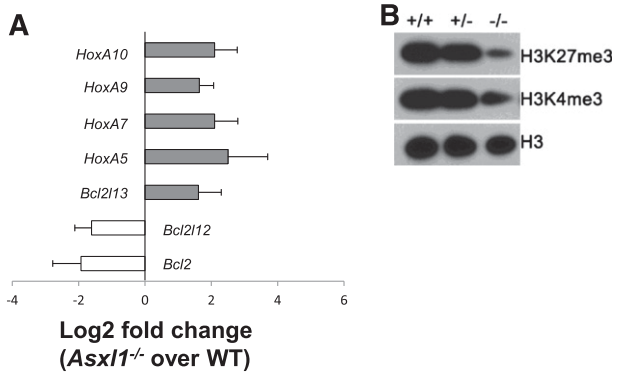

Figure 7. *Asxl1*$^{-/-}$ HSC/HPCs had an altered expression of genes implicated in apoptosis regulation and reduced global levels of H3K27me3 and H3K4me3. (A) The mRNA expression of *HoxA5/7/9/10, Bcl2l13, Bcl2,* and *Bcl2l12* in the BM Lin$^-$c-Kit$^+$ cells of WT (n = 4) and *Asxl1*$^{-/-}$ (n = 4) mice were determined by qPCR. Data are shown as relative expression units to the respective gene expression in WT mice using *Gapdh* as an internal calibrator. (B) Western blot analyses of H3K27me3 and H3K4me3 in the BM Lin$^-$c-Kit$^+$ cells of each genotype of mice. Total H3 levels served as loading controls. Representative blots from 3 independent experiments are shown.

observed an increased apoptosis and mitosis in *Asxl1*$^{+/-}$ and *Asxl1*$^{-/-}$ BM and Lin$^-$c-Kit$^+$ cells, which could result in the ineffective hematopoiesis and high risk of leukemic transformation in these mice. The upregulated apoptotic facilitator, *Bcl2l13*, and downregulated anti-apoptotic genes, *Bcl2* and *Bcl2l12,* in *Asxl1*$^{-/-}$ Lin$^-$c-Kit$^+$ cells could play a critical role in their increased apoptosis. Interestingly, myeloid progenitors of the *NUP98-HOXD13* transgenic MDS mice have been shown to have an increased rate of apoptosis, which is also associated with a reduction in *Bcl2*.[29]

Although truncated forms of the ASXL1 protein were undetectable in leukemia samples with *ASXL1* mutations in a recent study, suggesting that these mutations are likely loss-of-function disease alleles,[18] this still cannot definitively eliminate the possibility that truncated forms of ASXL1 resulting from *ASXL1* mutations in patients exert a gain-of-function and/or dominant-negative effect. In vivo studies using transgenic or knock-in strategies to express truncated Asxl1 proteins in mice are warranted to thoroughly clarify this possibility.

Aberrant apoptosis and/or senescence may alter the HSC/HPC pool in vivo. Indeed, *Asxl1*$^{-/-}$ mice had a decreased HSC pool. In a competitive reconstitution assay, *Asxl1*$^{-/-}$ HSC/HPCs exhibited a reduced HSC self-renewal and long-term hematopoietic repopulating capacity with a skewed cell differentiation, favoring granulocytic lineage. These data together with the increased apoptosis in *Asxl1*$^{-/-}$ HSC/HPCs suggest that Asxl1 regulates HSC/HPC cellular functions. The *ASXL1* gene can be translocated and fused to the *PAX5* gene in B-acute lymphoblastoid leukemia.[30] Recent genome sequencing studies revealed low frequencies of *ASXL1* mutations in B-chronic lymphocytic leukemia,[31] but not in T-cell–acute leukemia.[32] Although we did not observe lymphoid malignancies in the cohort of *Asxl1*$^{-/-}$ and *Asxl1*$^{+/-}$ mice, deletion/haploinsufficiency of *Asxl1* did cause impaired B-cell development, consistent with a previous report by Fisher et al.[23] Studies using B- or T-cell lineage–specific *Asxl1* inactivation may be necessary to further clarify the exact role of *Asxl1* in B- and T-cell development, respectively. Furthermore, increasing evidence has been shown that the BM microenvironment plays an important role in the development and progression of myeloid malignancies.[33] Our study cannot rule out a possibility that an altered microenvironment may contribute to the hematopoietic phenotype and myeloid malignancy development observed in the constitutive *Asxl1*-deficient murine models. However, the competitive transplantation data suggest an intrinsic effect of Asxl1 in regulating HSC/HPC function.

Interacting with histone-modifying enzymes including EZH2 and LSD1, *Asxl1* deletion globally decreases H3K27me3 and H3K4me3 in Lin$^-$c-Kit$^+$ cells, consistent with Abdel-Wahab et al's observation that *Asxl1* knockdown resulted in diminished H3K27me3 histone mark in leukemia myeloid cell lines.[18] H3K4me3 is associated with transcriptional competence and activation, whereas H3K27me3 and H3K9me3 are frequently associated with repressed gene expression.[34-37] It would be logical and important to interrogate the dysregulated gene expression with the genomic alteration of histone marks identified by Chip-Seq experiments.

Collectively, our results demonstrate that deletion/haploinsufficiency of *Asxl1* in mice is sufficient to recapitulate disease manifestations of patients with MDS and MDS/MPN, implying that Asxl1 functions as a tumor suppressor in myelopoiesis. The current *ASXL1* murine model provides an ideal platform for unveiling the detailed mechanisms of *Asxl1* loss–mediated multiple-step pathogenesis of myeloid malignancies and for testing novel therapeutic agents for myeloid malignant patients with *ASXL1* alterations.

Acknowledgments

This work was supported in part by grants from the Leukemia and Lymphoma Society (F.-C.Y.), the Department of Defense (NF073112 [F.-C.Y.]), the National Institutes of Health, National Cancer Institute (CA155294, [F.-C.Y.] and Heart, Lung and Blood Institute HL112294 [M.X.]), the Children's Tumor Foundation (S.R.), and the Indiana Clinical and Translational Sciences Institute (PHS NCCR, 5TL1RR025759-03 [S.D.R.]).

Authorship

Contribution: J.W., Z.L., Y.H., S.C., S.R., F.P., J.Y., L.J., L.N., and X.Y. performed the experiments and analyzed the data; Z.L. assisted in the statistical analysis; H.N. and J.Z. reviewed the blood smears and histopathologic sections; O.W. and C.-L.C. provided assistance in designing the study and revised the manuscript; and M.X. and F.-C.Y. designed and supervised the studies, performed the experiments, analyzed data, wrote the manuscript, and are responsible for its final draft.

Conflict-of-interest disclosure: The authors declare no competing financial interests.

Correspondence: Feng-Chun Yang, Department of Pediatrics, Herman B. Wells Center for Pediatric Research, Indiana University School of Medicine, 1044 W Walnut St, R4, Room 427, Indianapolis, IN 46202; e-mail: fyang@iu.edu; or Mingjiang Xu, Department of Pediatrics, Herman B. Wells Center for Pediatric Research, Indiana University School of Medicine, 1044 W Walnut St, R4, Room 119, Indianapolis, IN 46202; e-mail: mx2@iu.edu.

References

1. Fisher CL, Berger J, Randazzo F, Brock HW. A human homolog of Additional sex combs, ADDITIONAL SEX COMBS-LIKE 1, maps to chromosome 20q11. *Gene.* 2003;306:115-126.
2. LaJeunesse D, Shearn AE. E(z): a polycomb group gene or a trithorax group gene? *Development.* 1996;122(7):2189-2197.
3. Milne TA, Sinclair DA, Brock HW. The Additional sex combs gene of Drosophila is required for activation and repression of homeotic loci, and interacts specifically with Polycomb and super sex combs. *Mol Gen Genet.* 1999;261(4-5):753-761.
4. Lee SW, Cho YS, Na JM, et al. ASXL1 represses retinoic acid receptor-mediated transcription through associating with HP1 and LSD1. *J Biol Chem.* 2010;285(1):18-29.
5. Fisher CL, Randazzo F, Humphries RK, Brock HW. Characterization of Asxl1, a murine homolog of Additional sex combs, and analysis of the Asx-like gene family. *Gene.* 2006;369: 109-118.
6. Carbuccia N, Trouplin V, Gelsi-Boyer V, et al. Mutual exclusion of ASXL1 and NPM1 mutations in a series of acute myeloid leukemias. *Leukemia.* 2010;24(2):469-473.
7. Gelsi-Boyer V, Trouplin V, Adélaïde J, et al. Mutations of polycomb-associated gene ASXL1 in myelodysplastic syndromes and chronic myelomonocytic leukaemia. *Br J Haematol.* 2009; 145(6):788-800.
8. Boultwood J, Perry J, Pellagatti A, et al. Frequent mutation of the polycomb-associated gene ASXL1 in the myelodysplastic syndromes and in acute myeloid leukemia. *Leukemia.* 2010;24(5): 1062-1065.
9. Carbuccia N, Murati A, Trouplin V, et al. Mutations of ASXL1 gene in myeloproliferative neoplasms. *Leukemia.* 2009;23(11):2183-2186.
10. Boultwood J, Perry J, Zaman R, et al. High-density single nucleotide polymorphism array analysis and ASXL1 gene mutation screening in chronic myeloid leukemia during disease progression. *Leukemia.* 2010;24(6):1139-1145.
11. Sugimoto Y, Muramatsu H, Makishima H, et al. Spectrum of molecular defects in juvenile myelomonocytic leukaemia includes ASXL1 mutations. *Br J Haematol.* 2010;150(1):83-87.
12. Makishima H, Jankowska AM, McDevitt MA, et al. CBL, CBLB, TET2, ASXL1, and IDH1/2 mutations and additional chromosomal aberrations constitute molecular events in chronic myelogenous leukemia. *Blood.* 2011;117(21): e198-e206.
13. Gelsi-Boyer V, Trouplin V, Roquain J, et al. ASXL1 mutation is associated with poor prognosis and acute transformation in chronic myelomonocytic leukaemia. *Br J Haematol.* 2010; 151(4):365-375.
14. Bejar R, Stevenson K, Abdel-Wahab O, et al. Clinical effect of point mutations in myelodysplastic syndromes. *N Engl J Med.* 2011; 364(26):2496-2506.
15. Brecqueville M, Rey J, Bertucci F, et al. Mutation analysis of ASXL1, CBL, DNMT3A, IDH1, IDH2, JAK2, MPL, NF1, SF3B1, SUZ12, and TET2 in myeloproliferative neoplasms. *Genes Chromosomes Cancer.* 2012;51(8):743-755.
16. Stein BL, Williams DM, O'Keefe C, et al. Disruption of the ASXL1 gene is frequent in primary, post-essential thrombocytosis and post-polycythemia vera myelofibrosis, but not essential thrombocytosis or polycythemia vera: analysis of molecular genetics and clinical phenotypes. *Haematologica.* 2011;96(10):1462-1469.
17. Gelsi-Boyer V, Brecqueville M, Devillier R, Murati A, Mozziconacci MJ, Birnbaum D. Mutations in ASXL1 are associated with poor prognosis across the spectrum of malignant myeloid diseases. *J Hematol Oncol.* 2012;5:12.
18. Abdel-Wahab O, Adli M, LaFave LM, et al. ASXL1 mutations promote myeloid transformation through loss of PRC2-mediated gene repression. *Cancer Cell.* 2012;22(2):180-193.
19. Hoischen A, van Bon BW, Rodríguez-Santiago B, et al. De novo nonsense mutations in ASXL1 cause Bohring-Opitz syndrome. *Nat Genet.* 2011; 43(8):729-731.
20. Scheuermann JC, de Ayala Alonso AG, Oktaba K, et al. Histone H2A deubiquitinase activity of the Polycomb repressive complex PR-DUB. *Nature.* 2010;465(7295):243-247.
21. Cho YS, Kim EJ, Park UH, Sin HS, Um SJ. Additional sex comb-like 1 (ASXL1), in cooperation with SRC-1, acts as a ligand-dependent coactivator for retinoic acid receptor. *J Biol Chem.* 2006;281(26):17588-17598.
22. Fisher CL, Pineault N, Brookes C, et al. Loss-of-function Additional sex combs like 1 mutations disrupt hematopoiesis but do not cause severe myelodysplasia or leukemia. *Blood.* 2010;115(1): 38-46.
23. Fisher CL, Lee I, Bloyer S, et al. Additional sex combs-like 1 belongs to the enhancer of trithorax and polycomb group and genetically interacts with Cbx2 in mice. *Dev Biol.* 2010;337(1):9-15.
24. Kogan SC, Ward JM, Anver MR, et al; Hematopathology subcommittee of the Mouse Models of Human Cancers Consortium. Bethesda proposals for classification of nonlymphoid hematopoietic neoplasms in mice. *Blood.* 2002; 100(1):238-245.
25. Nimer SD. Myelodysplastic syndromes. *Blood.* 2008;111(10):4841-4851.
26. Simon JA, Tamkun JW. Programming off and on states in chromatin: mechanisms of Polycomb and trithorax group complexes. *Curr Opin Genet Dev.* 2002;12(2):210-218.
27. Thol F, Friesen I, Damm F, et al. Prognostic significance of ASXL1 mutations in patients with myelodysplastic syndromes. *J Clin Oncol.* 2011; 29(18):2499-2506.
28. Bouscary D, Chen YL, Guesnu M, et al. Activity of the caspase-3/CPP32 enzyme is increased in "early stage" myelodysplastic syndromes with excessive apoptosis, but caspase inhibition does not enhance colony formation in vitro. *Exp Hematol.* 2000;28(7): 784-791.
29. Slape CI, Saw J, Jowett JB, et al. Inhibition of apoptosis by BCL2 prevents leukemic transformation of a murine myelodysplastic syndrome. *Blood.* 2012;120(12):2475-2483.
30. An Q, Wright SL, Moorman AV, et al. Heterogeneous breakpoints in patients with acute lymphoblastic leukemia and the dic(9;20)(p11-13; q11) show recurrent involvement of genes at 20q11.21. *Haematologica.* 2009;94(8): 1164-1169.
31. Quesada V, Conde L, Villamor N, et al. Exome sequencing identifies recurrent mutations of the splicing factor SF3B1 gene in chronic lymphocytic leukemia. *Nat Genet.* 2012;44(1):47-52.
32. Zhang J, Ding L, Holmfeldt L, et al. The genetic basis of early T-cell precursor acute lymphoblastic leukaemia. *Nature.* 2012;481(7380):157-163.
33. Raaijmakers MH, Mukherjee S, Guo S, et al. Bone progenitor dysfunction induces myelodysplasia and secondary leukaemia. *Nature.* 2010; 464(7290):852-857.
34. Barski A, Cuddapah S, Cui K, et al. High-resolution profiling of histone methylations in the human genome. *Cell.* 2007;129(4): 823-837.
35. Bernstein BE, Mikkelsen TS, Xie X, et al. A bivalent chromatin structure marks key developmental genes in embryonic stem cells. *Cell.* 2006;125(2):315-326.
36. Mikkelsen TS, Ku M, Jaffe DB, et al. Genome-wide maps of chromatin state in pluripotent and lineage-committed cells. *Nature.* 2007;448(7153): 553-560.
37. Guenther MG, Levine SS, Boyer LA, Jaenisch R, Young RA. A chromatin landmark and transcription initiation at most promoters in human cells. *Cell.* 2007;130(1):77-88.